Chaudhary et al., J Material Sci Eng 2017, 6:3
DOI: 10.4172/2169-0022.1000339

Journal of Material Sciences & Engineering

Research Article OMICS International

Electrical Resistivity Change of SeTeAg Compositions to Thermal and Pressure as Stress

Chaudhary N[1], Prasad KNN[2] and Goyal N[1]*

[1]Department of Physics, Punjab University, Chandigarh, India
[2]Department of Physics, BNM Institute of Technology, Bangalore, India

Abstract

To understand the behaviour of materials for applications in solid state electronic devices, the materials are to be exposed to different stresses such as thermal, electrical, humidity, optical, nuclear radiations, pressure (static or dynamic) etc. to better understand their structural, morphology, conduction, optical and sensing properties. The Se85-xTe15Agxcompositions prepared from melt-quench technique were exposed to high pressure (0-10 GPa) and temperature (300-373 K). The results depict the change in resistivity with respect to pressure in forward as well as backward pressurization. These results depicts that there is very small change in resistivity with change in pressure and the change in resistivity with respect to pressure follows the same pattern, when the pressure is applied from atmospheric pressure to 10 GPa and vice versa. The results of resistivity change with the variation of Silver in the compositions are also reported in this study. Similar results are observed in case of resistivity change with respect to temperature. Some deviation is observed in the results which are well explained with average coordination number, fermi level change and crystallinity.

Keywords: Semiconductor; Diffraction; Resistivity; Nano crystallization

Introduction

Ternary semiconductors based on Selenium Tellurium doped with metals are widely used in fabrication of electronic devices. Various researchers have studied the optical, thermal and dielectric properties of amorphous semiconductors. But, still a lot is to be known yet for Nano crystalline semiconductors to facilitate these materials to be used in Low Power Electronics. Chalcogenide semiconductors are nowadays widely used in medical, defense and consumer electronics as applied to the fields of xerography, holography, optical sensors and filters, waveguides, industrial switches and many more applications [1,2]. Thin films of chalcogens are more prominently used in Infra-red optics as these help in energy management and night vision [3]. Selenium Telluride binary and ternary alloys are best suited for thermal imaging i.e. detection of human body in the darkness as at room temperature human body emits radiations in 8-12 μm. Region and Selenium Telluride compositions have the same absorption region; hence can help to detect the presence of human body in darkness [4]. Chalcogenide optical fibers are also used in low power transmission. These are further suitable in microsurgery and bio-sensing tumor, analyzing serum in medical field. IR camera technology is also the outcome of developments in the field of chalcogenide semiconductors. In normal conditions the electronic devices are commercially available but here the intention was to find the response of these materials under harsh conditions. Hence, studied the electrical behaviour under stresses (pressure and thermal). An approach is missing where the effect of different stresses on these materials is studied. This study reports the electrical resistivity change under pressure and temperature of $Se_{85-x}Te_{15}Ag_x$ [5]. The variation in properties under different stresses for different compositions specify that these materials can be of great use in fabrication of solid state electronic devices and pressure tolerant electronics [6].

Experimental Studies

Material preparation

Conventional technique of melting and then ice cooled quenching [7,8] is used to synthesize $Se_{85-x}Te_{15}Ag_x$ (x=0, 2, 6, 10, 15) material samples. For $Se_{85-x}Te_{15}Ag_x$ the pure elements {Selenium pellets 2N; Tellurium 2N and Silver powder 2N} were used. For required compositions the pure elements were weighed in required atomic weight percentages, using Wensar™ MAB220 model electronic weighing machine having resolution of 10^{-4} gm. $Se_{85-x}Te_{15}Ag_x$ were melted inside the furnace at 1250 K for nearly 24 hours in vacuum sealed Quartz ampoules (length-12 cm; internal dia. 8 mm and outer dia. 10 mm). The temperature for melting the mixed compositions was decided on the basis of value of maximum melting point of the elements used for the compositions. In case of $Se_{85-x}Te_{15}Ag_x$ the highest melting point is of Silver (1234.93 K) hence, melted inside the furnace at 1250 K. The melted compositions are then ice cooled and further powdered. The amorphous and crystalline nature of the samples was confirmed by powder X-ray Diffraction measurements.

Resistivity change measurement set-up

The compositions prepared from melt-quench technique were exposed to high pressure using Bridgman opposed anvil cell. Pyrophyllite gaskets of 0.35 mm critical thickness have been used in split gasket configuration. Steatite has been used as the quasi-hydrostatic pressure-transmitting medium [9-11]. A two probe method was employed for the electrical measurements; a current of 50 mA was passed through the sample using a constant current source and the voltage across sample was measured using a Keithley 614 nano-voltmeter. This nano-voltmeter works on principle of dual slope Analog to Digital Converter. This can detect current as low as 10^{-14} A having very high input impedance ($5 \times 10^{13}\Omega$).

***Corresponding author:** Prof. Navdeep Goyal, Department of Physics, Punjab University, Chandigarh-160014, India, Tel: 9464108429; E-mail: ngoyal@pu.ac.in.

Received April 28, 2017; **Accepted** May 18, 2017; **Published** May 28, 2017

Citation: Chaudhary N, Prasad KNN, Goyal N (2017) Electrical Resistivity Change of SeTeAg Compositions to Thermal and Pressure as Stress. J Material Sci Eng 6: 339. doi: 10.4172/2169-0022.1000339

To measure the DC conductivity and thermal activation energy of the sample, a constant DC voltage was applied across the sample (palette of 12 mm. dia. and 1 mm thickness) by Keithley 224 programmable power supply and the resulting current was measured using a Digital Picoammeter Model DPM-111 (Scientific Equipment Roorkee). The change in temperature was controlled at a rate of 1°C/min using a variac. The temperature was noted using (Audiotronics) a Temperature Controller (Figure 1).

Results and Discussion

Characterization

X-Ray diffraction pattern shown in Figure 2 confirms the amorphous nature of $Se_{85}Te_{15}$ and polycrystalline nature of $Se_{85-x}Te_{15}Ag_x$ (x=2, 6, 10 and 15) alloys which have sharp and clearly resolved peaks. These measurements were done using Cu K_α line radiation of wavelength 1.54 Å. The average size of the crystallite was determined using Debye-Scherrer's formula: $D=0.9\lambda/\beta\cos\theta$ where β is the full width at half maximum (FWHM) of the peak, λ is X-ray wavelength, θ is the Bragg angle [12-15]. The average crystallite sizes of prepared compounds are less than 100 nm The average crystallite size and symmetry with lattice constants of prepared compounds is given in the Table 1. Lattice constants were determined using Powder XRD/Expert Hi-Score software. The analysis of XRD clarifies the tetragonal structures of both the compositions. There is not much variation in the average size of the crystals formed.

Resistivity change under pressure

The results shown in Figure 3 depict the change in resistivity w.r.t. pressure in forward as well as backward pressurization for $Se_{85}Te_{15}$ and Figure 4 represents the resistivity change w.r.t. pressure in forward as well as backward pressurization for ternary Nano crystalline materials $Se_{85-x}Te_{15}Ag_x$ (x=2, 6, 10, 15). These results depict that there is very small change in resistivity with change in pressure and the change in resistivity w.r.t. pressure follows the same pattern, when the pressure is applied from atmospheric pressure to 10 GPa and vice versa. Figure 5 presents ternary Nano crystalline material $Se_{83}Te_{15}Ag_2$; $Se_{79}Te_{15}Ag_6$; $Se_{75}Te_{15}Ag_{10}$ and $Se_{70}Te_{15}Ag_{15}$. The graph shows that at room temperature the materials show very less resistivity change even at high pressure i.e. 10 GPa. The change can be calculated by subtracting resistivity value at 10 GPa and at atmospheric pressure. This difference can be divided by the original resistivity value (at atmospheric pressure) and multiplied by 100 to get the percentage resistivity change. Table 2 reports the percentage change in the resistivity.

The results of resistivity change percentage clarifies that the addition of Silver makes the material more stable and the stress leads to almost negligible amount of resistivity change. The result can be interpreted in relation to Young's modulus. The values of Young's modulus for Selenium, Tellurium and Silver are 10 GPa, 43 GPa and 82.7 GPa respectively [16]. The ternary material prepared is showing negligible resistance change even under 10 GPa pressure, justifying that there is negligible amount of change in the dimensions of the sample.

Further the variation in resistivity change with the variation in Silver in the compositions can be related to cross linking and rigidity [17] which is dependent on average coordination number as well. The mean coordination number (N_c) values tabulated in Table 3 for the investigated ternary glassy alloy $Se_xTe_yAg_z$ (x+y+z=1), are calculated using the equation $Nc=xCN(Se)+yCN(Te)+zCN(Ag)$; [18] where CN is the coordination number of the specific element (Se=2; Te=2 and Ag=4) and x, y and z are the atomic concentrations of Se, Te and Ag, respectively. The physical properties' dependence on average coordination number is well studied by various researchers [19-21]. Several researchers reported the threshold compositions at different average coordination numbers and settled at a viewpoint that threshold value may lie between 2 and 3 for different elements [22]. With increase

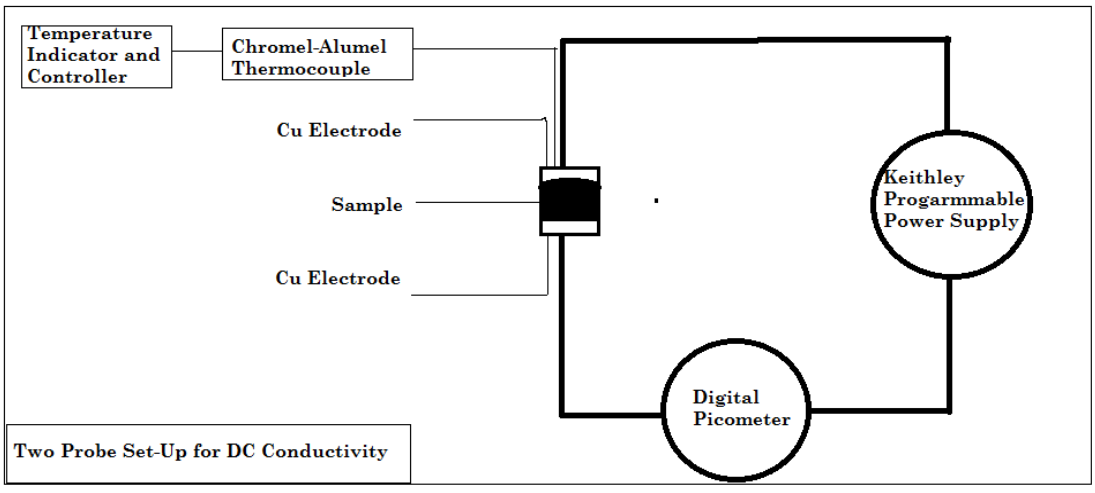

Figure 1: DC conductivity measurement set-up.

Sample Name	Symmetry	a	b	c	Average Crystallite size (nm)
$Se_{70}Te_{15}Ag_{15}$	Tetragonal	6.55209	6.55209	18.65308	36.25
$Se_{75}Te_{15}Ag_{10}$	Tetragonal	6.55110	6.55110	18.64573	37.61
$Se_{79}Te_{15}Ag_6$	Tetragonal	6.55941	6.55941	18.60991	32.55
$Se_{83}Te_{15}Ag_2$	Tetragonal	6.54574	6.54574	18.65955	37.36

Table 1: Average crystallite size and symmetry with lattice constants of $Se_{85-x}Te_{15}Ag_x$.

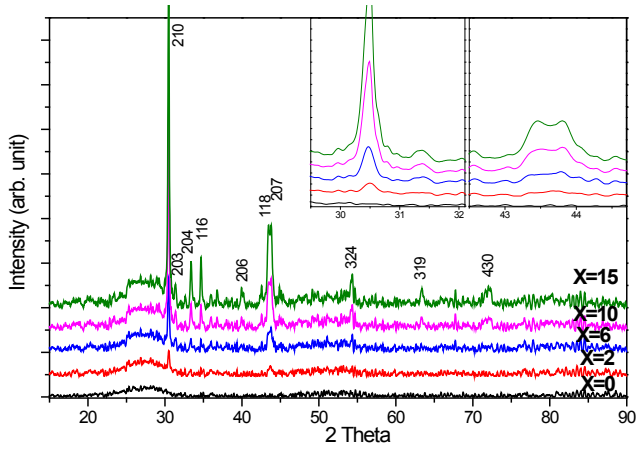

Figure 2: XRD of Se85-xTe15Agx (x=0, 2, 6, 10, and 15) bulk form.

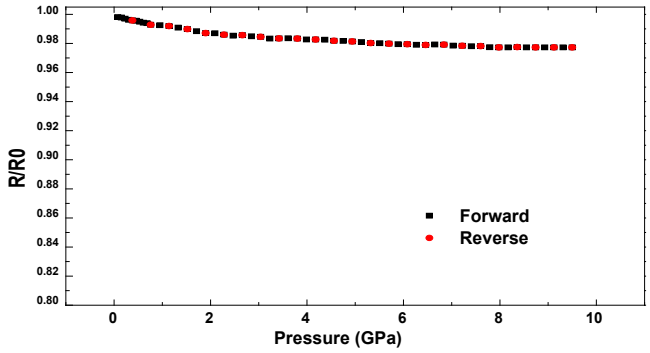

Figure 3: Resistivity change w.r.t. pressure in forward as well as backward pressurization for $Se_{85}Te_{15}$.

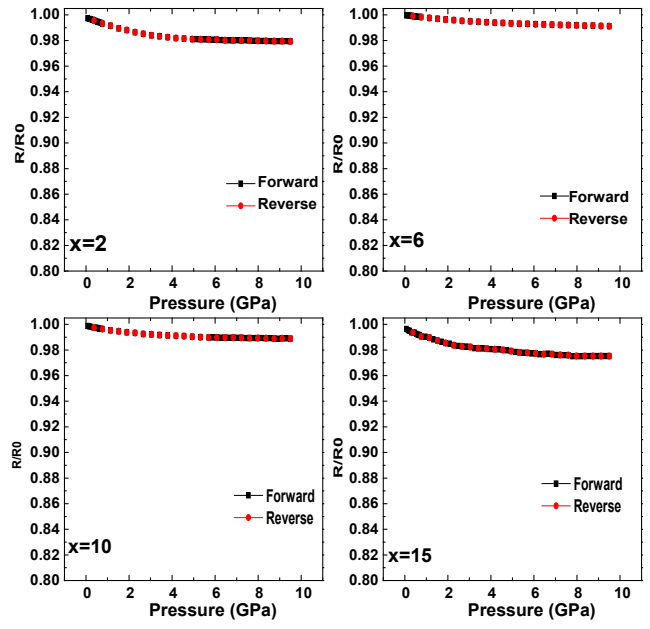

Figure 4: Resistivity change w.r.t. pressure in forward as well as backward pressurization for ternary nanocrystalline materials $Se_{85-x}Te_{15}Ag_x$ (x=2, 6, 10, 15).

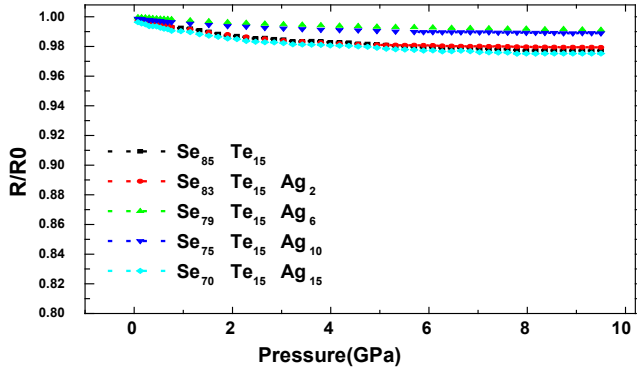

Figure 5: Resistivity change of amorphous $Se_{85}Te_{15}$ and ternary nanocrystalline materials $Se_{85-x}Te_{15}Ag_x$ (x=0, 2, 6, 10, 15).

$Se_{85-x}Te_{15}Ag_x$ (x=0, 2, 6, 10, and 15)		
x	**Coordination number**	**Percentage change in the resistivity**
0	2.00	2.09
2	2.04	1.81
6	2.12	0.85
10	2.20	0.99
15	2.30	2.12

Table 2: Values of average coordination number and percentage change in resistivity in $Se_{85-x}Te_{15}Ag_x$ (x=0, 2, 6, 10, and 15) and $Se_{85-x}Te_{15}Ga_x$ (x=0, 2, 6, 10, and 15) compositions.

x	E_a 300K-345K (eV)	E_a 345K-373K (eV)	E_a 300K-373K (eV)	σ_{dc}(S/m)	$\sigma_{0\ (Ohm^{-1}m^{-1})}$	Coordination number
0	1.46	0.50	0.98	9.97E-9	4.12E-7	2.00
2	2.24	0.33	0.86	1.55E-7	1.26E-5	2.04
6	1.46	0.31	0.73	1.21E-6	7.09E-7	2.12
10	0.11	0.11	0.05	0.010	0.01	2.20
15	0.20	0.20	0.11	0.016	0.06	2.30

Table 3: Values of Thermal Activation Energy (E_a), Pre-exponential factor (σ_0), DC Conductivity (σdc) and Coordination No. (Z) for $Se_{85\_x}Te_{15}Ag_x$ (x =0, 2, 6, 10 and 15).

in average coordination number due to addition of third element in Selenium Telluride, cross-linking and rigidity increases which further increases glass transition temperature as well as resistivity [23].

With the increase in Silver content the compositions, become more rigid and better cross linked and dense as the coordination number is increasing. Structures of multicomponent systems are associated with average coordination number and it is highly composition dependent. Due to this, increase in pressure is not causing the change in its resistivity. In case of Silver as additive in SeTe, as the concentration of Ag increases the change in resistivity with pressure decreases upto x=6 in $Se_{85-x}Te_{15}Ag_x$ (x=2, 6, 10, 15) compositions. But as the concentration of Ag increases further the change in resistivity with pressure again increases. The threshold values of coordination number for ternary semiconductors vary with the additive elements. In the studied compositions, the increase in the coordination number up to 2.2 exhibits reversal in the property. Moreover, with Silver as additive when it exceeds x=6 in the studied compositions it leads to increase in crystallinity evident from Figure 2 may also be attributed for the reversal in the property.

Resistivity change w.r.t. pressure in forward as well as backward pressurization for ternary nanocrystalline materials $Se_{85-x}Te_{15}Ag_x$ (x=2, 6, 10, 15) shows no change (Figure 3) depicts that there is no structural

change in the material with pressurization even up to 10 GPa as the forward and reverse plots follow the same path.

Resistivity change under temperature

The resistivity change of $Se_{85-x}Te_{15}Ag_x$ (x=2, 6, 10 and 15) w.r.t to temperature (Figure 6) also shows a variation for different compositions. As the Silver content increases resistivity change decreases. The results are similar to resistivity change w.r.t pressure and justifying the fact that with the increase of coordination number. This also supports that with increase in the crystallinity (Figure 2) of the material less change is observed in the conductivity change even at higher temperatures. But the trend is reversed for higher concentration of Silver in the compositions as observed in the behaviour for pressure as stress. This is because of the threshold value in the coordination number in the compositions it shows reversal in the pattern of the observed property similar to the results observed for resistivity change due to pressure.

The temperature dependence plots of D.C. conductivity for $Se_{85-x}Te_{15}Ag_x$ (Figure 6) are straight lines having two slopes for x=0, 2, 6. It signifies that the D.C. conductivity is due to thermally activated process having two activation energy levels i.e. two conduction mechanisms in the measuring range of temperature. With decrease in temperature electrical conductivity decreases which corresponds to its hopping conduction mechanism. This region lies from 300-345 K. In the temperature region 345-373 K, with increase in temperature conductivity increases refers tunnelling of carriers either in localized states in the band tails or in extended states. In semiconductors conduction mechanism depends on the values of pre-exponential factor (σ_0).The range 10^5-10^6 $\Omega^{-1}m^{-1}$ indicates conduction in extended states, but the calculated values of pre exponential factor are three to four orders lesser than 10^5-10^6 $\Omega^{-1}m^{-1}$ range. Henceforth, there is no chance of conduction in extended states but, there is most likely existence of wide range of localized states. Therefore, there is the possibility of conduction in localized states in band tails. The activation energy is calculated using Arrhenius equation $\left(\sigma = \sigma 0 \exp\left(-\frac{\Delta Ea}{KT}\right)\right)$. The values of ΔE_a were calculated using the slopes of the curves of Figure 7 and pre-exponential factor is calculated from intercept on y-axis in Arrhenius plots. The results are tabulated in Table 3. For the studied samples ΔE_a is highly composition dependent. The values of ΔE_a, decreases and DC conductivity increases as the Ag concentration increases (Figure 8). This increase of DC conductivity and decrease in thermal activation energy is because of shift of Fermi level in impurity doped chalcogenide

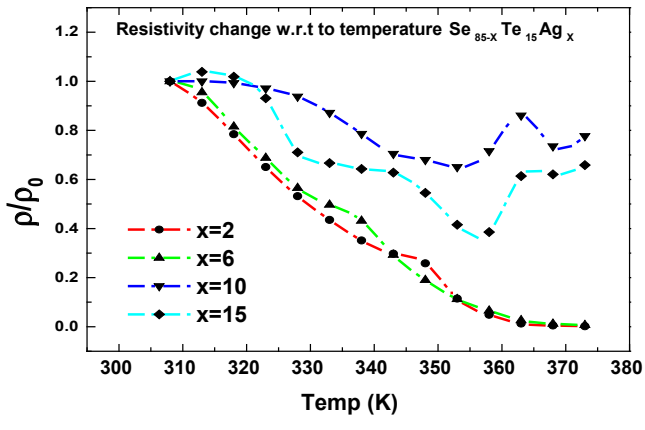

Figure 6: Resistivity change w.r.t to Temperature for $Se_{85-x}Te_{15}Ag_x$ (x=2, 6, 10, 15).

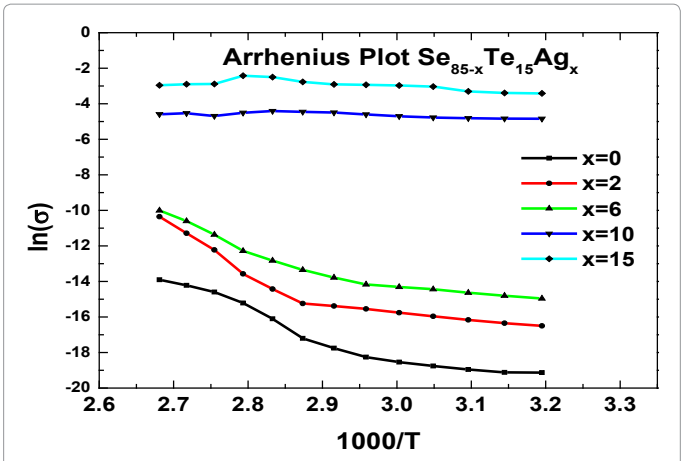

Figure 7: Temperature dependence of dc electrical conductivity for $Se_{85-x}Te_{15}Ga_x$ (x =0, 2, 6, 10 and 15).

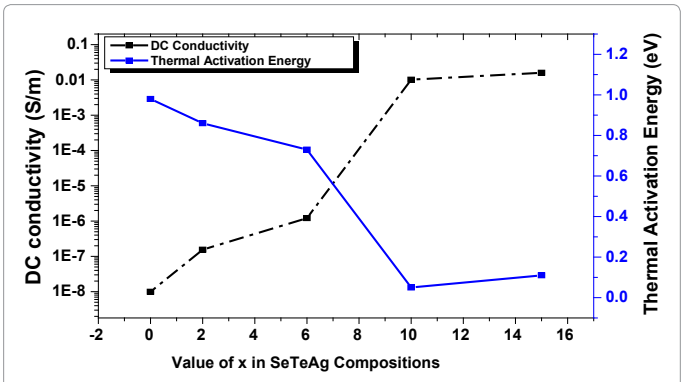

Figure 8: DC Conductivity and Activation Energy variation with Ag content.

semiconductors [24]. The addition of conductive dopant might have the potency to increase the concentration of charge carriers which shift the Fermi level [25-28]. In case of x=10 and 15 the slope of Arrhenius plot is very small, giving very small thermal activation energy. Being Silver a very conductive element large shift in the Fermi level is expected.

Conclusion

From the results achieved it is concluded that these materials can be best suited for the applications where electronic devices are to be fabricated for high pressure applications. In high pressure environment, where it is required, that the material do not change its conductivity w.r.t. pressure, these materials can find their application. Negligible amount of change is observed when Silver is in small content in the compound. But with the increase in Silver the change in resistivity is reduced significantly. Effect of Silver is explained with its increased cross linking capability in the material. But the reversal is observed in resistivity change pattern as the coordination number achieves certain threshold value in the compositions.The detailed study of temperature dependent DC electrical conductivity of bulk nanocrystalline SeTeAg system elaborated that with increase in Silver the change in resistivity is less due to change in the Fermi level upto x=10. Beyond that the trend is reversed due to threshold achieved in the compositions. Thermal activation energy increased with addition of Silver attributed to the fact that Silver introduces better cross-linked structures but further increase in Silver reduces the thermal activation energy because of increase in concentration of carriers. Further at higher temperatures tunnelling of

carriers in localized states in the band tails is suggested as calculated values of pre-exponential factor are very small.

References

1. Elabbar AA (2009) Kinetics of the glass transition in Se 72 Te 23 Sb 5 chalcogenide glass: Variation of the activation energy. Journal of Alloys and Compounds 476: 125-129.
2. Deepika C, Jain PK, Rathore KS, Saxena NS (2009) J Non-Cryst Solids 355: 1274-1280.
3. Johnson RB (1998) Proc Soc Photo-Optical Instrumentation Engrs, SPIE 915: 106.
4. Hilton AR, Jones CE, Brau M (1966) Non-Oxide IVA-VA-VIA Chalcogenide Glasses. I. Glass-Forming Regions and Variations in Physical Properties. Physics and Chemistry of Glasses 7: 105.
5. Khan SA, Al-Hazmi FS, Faidah AS, Al-Ghamdi AA (2009) Calorimetric studies of the crystallization process in a-Se 75 S 25-xAgx chalcogenide glasses. Current Applied Physics 9: 567-572.
6. Pittini R, Hernes M (2012) Pressure-Tolerant Power Electronics for Deep and Ultradeep Water. Oil and Gas Facilities 1: 47-52.
7. Wang Y, Ohata E, Hosokawa S, Sakurai M, Matsubara E (2004) Intermediate-range order in glassy Ge x Se 1-x around the stiffness transition composition. Journal of Non-crystalline Solids 337: 54-61.
8. Khan ZH, Zulfequar M, Ilyas M, Husain M, Begum KS (2002) Electrical and thermal properties of a-(Se 70 Te 30) 100-x (Se 98 Bi 2) x (0⩽ x⩽ 20) alloys. Current Applied Physics 2: 167-174.
9. Bandyopadhyay AK, Nalini AV, Gopal ESR, Subramanyam SV (1980) High pressure clamp for electrical measurements up to 8 GPa and temperature down to 77 K. Review of Scientific Instruments, 51: 136-139.
10. Klement Jr W, Jayaraman A, Kennedy GC (1963) Phase Diagrams of Arsenic, Antimony, and Bismuth at Pressures up to 70 kbars. Physical Review 131: 632.
11. http://en.wikipedia.org/wiki/Selenium,http://en.wikipedia.org/wiki/Tellurium
12. Harnwell GP, Livingood JJ (1933) Experimental atomic physics. Mcgraw-Hill Book Company, Inc., London.
13. Nuffield EW (1966) X-ray diffraction methods.
14. Woolfson MM, Robinson I (1997) An Introduction to X-Ray Crystallography.
15. Bradley CC (1969) High pressure methods in solid state research.
16. http://en.wikipedia.org/wiki/Gallium
17. Saxena M, Agarwal MK, Kukreti AK, Rastogi N (2012) Effect on physical properties of Ge20Se80-xGax glass system with compositional variations. Advances in Applied Science Research 3: 1440-1448.
18. Chicago TS (1959) Mass, Optical Properties of Semiconductors. Butterworths scientific Publications, London.
19. Phillips JC (1979) Topology of covalent non-crystalline solids I: Short-range order in chalcogenide alloys. Journal of Non-Crystalline Solids 34: 153-181.
20. Thorpe MF (1983) Continuous deformations in random networks. Journal of Non-Crystalline Solids 57: 355-370.
21. Tanaka K (1989) Structural phase transitions in chalcogenide glasses. Physical Review B 39: 1270.
22. Saffarini G, Saiter JM (2006) Compactness in relation to the mean coordination number in glassy GexBi6S94-x. Chalcogenide Lett 3: 49-53.
23. Sarrach DJ, De Neufville JP, Haworth WL (1976) Studies of amorphous Ge Se Te alloys (I): Preparation and calorimetric observations. Journal of Non-Crystalline Solids 22: 245-267.
24. Elliott SR (1978) Defect states in amorphous silicon. Philosophical Magazine B 38: 325-334.
25. Malik MM, Zulfequar M, Kumar A, Husain M (1992) Effect of indium impurities on the electrical properties of amorphous Ga30Se70. Journal of Physics: Condensed Matter 4: 8331.
26. Okano S (1983) J Non-Crystalline Solids 50: 969-972.
27. Arora R, Tripathi SK, Kumar A (1990) Electrical conductivity and dielectric relaxation in bulk glassy Se 80-x Te 20 In x. Journal of materials science letters 9: 348-350.
28. Shimakawa K (1982) On the temperature dependence of ac conduction in chalcogenide glasses. Philosophical Magazine B 46: 123-135.

Citation: Chaudhary N, Prasad KNN, Goyal N (2017) Electrical Resistivity Change of SeTeAg Compositions to Thermal and Pressure as Stress. J Material Sci Eng 6: 339. doi: 10.4172/2169-0022.1000339